FEBS Letters 422 (1998) 36–42 FEBS 19742

Spermine binding to liver mitochondria deenergized by ruthenium red plus either FCCP or antimycin A

Lisa Dalla Via[b], Vito Di Noto[c], Antonio Toninello[a,*]

[a] *Dipartimento di Chimica Biologica, Università di Padova, Centro di Studio delle Biomembrane del CNR di Padova, viale G. Colombo 3, 35121 Padua, Italy*
[b] *Dipartimento di Scienze Farmaceutiche, Università di Padova, via Marzolo 5, 35121 Padua, Italy*
[c] *Dipartimento di Chimica Inorganica, Metallorganica ed Analitica, Università di Padova, via Loredan 4, 35121 Padua, Italy*

Received 17 November 1997

Abstract Thermodynamic analysis of spermine binding to mitochondria treated with ruthenium red and deenergized with either FCCP or antimycin A confirms the presence of two polyamine binding sites, S_1 and S_2, both with monocoordination, as previously observed in energized mitochondria [Dalla Via et al., Biochim. Biophys. Acta 1284 (1996) 247–252]. Both sites undergo a marked change in binding capacity and binding affinity upon mitochondrial deenergization. This change is most likely responsible for the incomplete or delayed spermine-mediated inhibition of the permeability transition induced in deenergized mitochondria.

Key words: Spermine; Binding site; Deenergized mitochondrion; Permeability transition

1. Introduction

Overloading of the mitochondrial matrix with Ca^{2+}, in combination with any of a wide variety of inducing agents, promotes a permeability transition of the inner mitochondrial membrane that results in a dramatic increase in permeability to molecules and ions up to 1500 Da in size. The final consequence of this process is the collapse of the proton electrochemical gradient paralleled by a shutdown of ATP synthesis and loss of control of matrix volume (for reviews see [1,2]).

The discovery that submicromolar concentrations of the immunosuppressant undecapeptide cyclosporin A (CsA) totally block this process [3,4] would be consistent with the operation of a proteinaceous pore, and suggests that it reflects the transformation of an ion-selective channel or the adenine nucleotide antiport to a non-specific pore [5,6] or the opening of a latent high resistance channel [7,8]. It has been proposed that outer membrane porin [9,10] or a complex of this protein with hexokinase and creatine kinase [11] might constitute the pore. The target of CsA seems to be a matrix cyclophilin [12], a member of the cyclophilin family of peptidyl-prolyl-*cis-trans*-isomerases. Notwithstanding the large number of papers published in the past decade, at present the molecular basis of the genesis of this process is not understood. Upon Ca^{2+} accumulation, the permeability transition can also be generated by substituting the classical inducer with an inhibitor of the Ca^{2+} uniporter such as ruthenium red plus an uncoupler [8,13,14]. Although the activity of ruthenium red as an inhibitor of reverse Ca^{2+} uniport remains controversial [13,15–17], it has been proposed that the following events are necessary to trigger the permeability transition: membrane depolarization [18], reverse Ca^{2+} uniport inhibition [19], prevention of matrix pH acidification [8] and binding of external divalent cations to a specific site [14].

Recently it has been demonstrated that the permeability transition promotes a loss of endogenous polyamines [20]. The presence of these polycations in the matrix space should be considered relevant and would be analogous to the activity of Mg^{2+} and adenine nucleotides in maintaining the energy barrier of liver mitochondria. Spermine prevents the permeability transition in energized liver [21–26] and heart mitochondria [23,27,28] upon induction by Ca^{2+} loading followed by addition of an inducer such as inorganic phosphate, *tert*-butyl-hydroperoxide, phenylarsine oxide, carboxyatractyloside or palmitoyl CoA. The sensitivity of the permeability transition of liver mitochondria to spermine depends on the ionic composition of the incubation medium [23]. Furthermore, spermine is also able to inhibit the permeability transition in liver mitochondria when the phenomenon is induced by ruthenium red plus FCCP [23]. The protective action of spermine resembles that of Mg^{2+} [29] but is much more effective because of its higher net positive charge [26]. The inhibitory mechanism of spermine is not known. It has been suggested that it might act by increasing the affinity of ADP for its inhibitory binding site [25]. Alternatively, the effect might be due to the binding of this polycation to an external site with a consequent change in the membrane surface potential [14]. Spermine-mediated inhibition of pore opening is usually achieved in energized mitochondria in which the polyamine is actively transported into the matrix space by a specific electrophoretic uniport [30,31]. However, the fact that spermine also protects against the permeability transition in deenergized mitochondria [23], in which spermine transport is almost completely inhibited [32], and the observation that K^+ interacts with a site outside the mitochondria to decrease spermine efficacy [23] strongly suggest that an external site is involved in this action.

By using a new thermodynamic treatment of ligand-receptor interactions [33], it has recently been demonstrated that two spermine binding sites are present in energized mitochondria [34]. The aim of the present study was to investigate whether the binding parameters and functional properties of the spermine binding sites are affected in mitochondria permeabilized by the concerted action of ruthenium red plus either FCCP or antimycin A.

*Corresponding author. Fax: (39) (49) 8073310.
E-mail: toninell@civ.bio.unipd.it

PII S0014-5793(97)01594-9

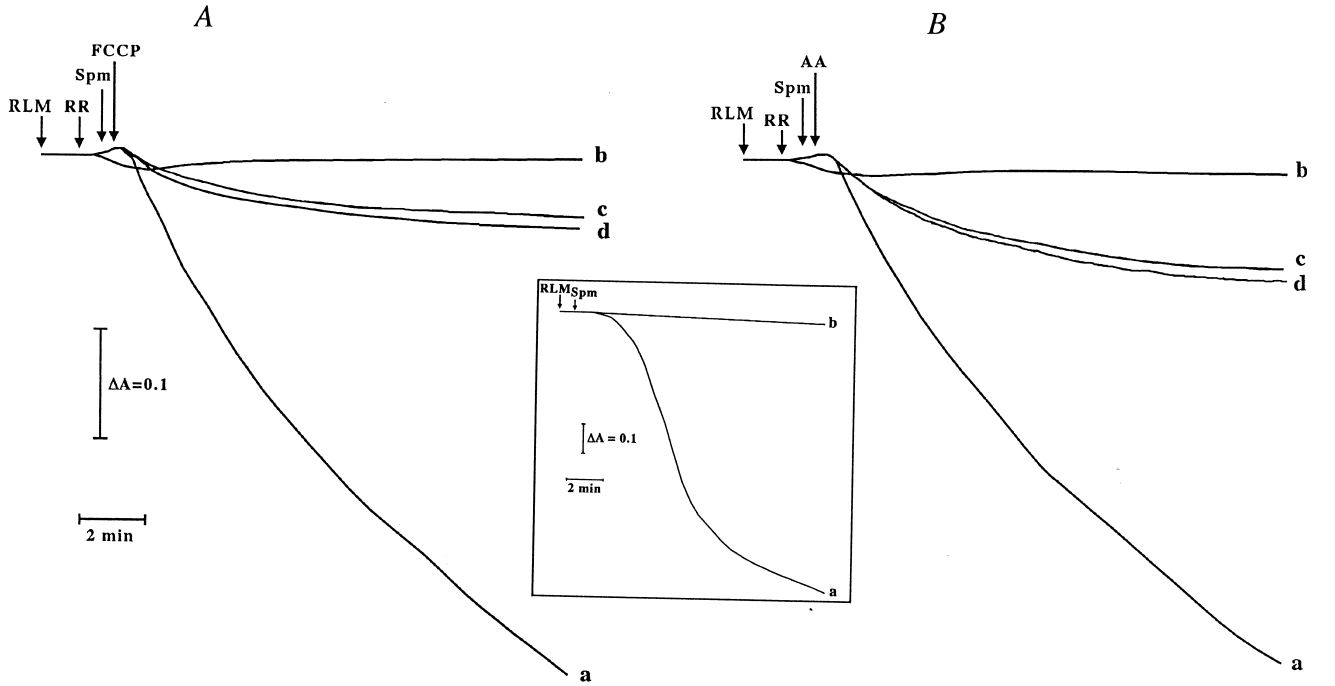

Fig. 1. Effect of spermine on the permeability transition induced by ruthenium red plus FCCP (panel A) or ruthenium red plus antimycin A (panel B). Rat liver mitochondria (RLM) were incubated in standard medium under the conditions described in Section 2. FCCP (0.2 μM) or antimycin A (AA, 45 nM) was added as indicated (traces a–d of the respective panels). Spermine (Spm) was added to a final concentration of 100 μM (traces c) or 250 μM (traces d). Ruthenium red (RR, 1 μM) was present in traces a, c and d of both panels. The inset shows the effect of 50 μM spermine (trace b) on the permeability transition induced by 100 μM Ca^{2+} plus 3 mM phosphate (trace a). These experiments were performed 10 times with identical results.

2. Materials and methods

Rat liver mitochondria were isolated in 0.25 M sucrose and 5 mM HEPES (pH 7.4) by conventional differential centrifugation.

Protein concentration was assayed by the biuret reaction with bovine serum albumin as a standard.

All incubations were conducted at 20°C with 1 mg of mitochondrial protein/ml in a low ionic strength medium, condition used in previous permeability transition [8,20,24,26], spermine binding [34] and spermine transport [30–32] studies. The medium contained 200 mM sucrose, 10 mM HEPES (pH 7.4), 5 mM sodium succinate, 1.25 μM rotenone and 1 mM sodium phosphate. In all experiments 100 μM $CaCl_2$ was present. Modifications of the standard medium are indicated in the figure legends.

Crude ruthenium red was purchased from Sigma and used without purification as previously suggested [35].

Mitochondrial swelling was monitored by apparent absorbance measurements at 540 nm in a Kontron Uvikon-922 spectrophotometer equipped with a magnetic stirrer and thermostatic control.

Uptake of [^{14}C]spermine was determined by a centrifugal filtration method as previously described [30,32].

Binding parameters were calculated as previously reported for energized mitochondria [34] by applying a new thermodynamic treatment of ligand-receptor interactions [33]. Scatchard and Hill analyses were performed using equations 1 and 2, respectively:

$$\frac{[B]}{[F]} = \sum_{i=1}^{s} \left\{ [B_{\max,i}] - [B_i] \right\} \cdot \left[\frac{1}{K_{i,1}(t)} + \varepsilon_i(F) \right] \quad (1)$$

$$\ln\left\{ \frac{[B]}{[B_{\max}] - [B]} \right\} = \ln\left\{ \sum_{i=1}^{s} x_i(F) \left[\frac{1}{K_{i,1}(t)} + \varepsilon_i(F) \right] \right\} + \ln[F] \quad (2)$$

where

$$\varepsilon_i(F) = \sum_{k=2}^{n_i} \frac{[F]^{k-1}}{\prod_{j=1}^{k} K_{i,j}(t)}$$

represents the appropriate measure of the extent of multiple coordination on the i-th site. $[B_{\max,i}]$is the maximum concentration of i-th sites that may be bound by the ligand, $[B_i]$ is the concentration of i-th sites bound by the ligand, $[B_{\max}]$ is the maximum receptor-bonded ligand concentration, and $[B]$ is the receptor-bonded ligand concentration. $[F]$ is the free ligand concentration, $K_{i,j}(t)$ is the affinity constant of the ligand for the i-th site, j is the occupancy number and t is time.

Fitting was performed using a FORTRAN program developed in our laboratory as described in [33].

The distribution of total bound spermine on its respective binding sites was calculated by parameter $X_i(F)$ obtained by means of equation 3:

$$X_i(F) = \frac{[B_{\max,i}] - [B_i]}{[B_{\max}] - [B]} = \frac{1}{1 + \beta_i[F]} \quad (3)$$

where the quantity is a parameter that describes the influence of the parallel filling of the other k-th sites in comparison to filling of the i-th site [33].

3. Results

The results reported in Fig. 1 show that treatment of respiring mitochondria in a standard sucrose-containing medium with ruthenium red followed by FCCP (panel A) or antimycin A (panel B) produces an apparent decrease in absorbance at 540 nm (traces a in both panels). This change in absorbance is indicative of mitochondrial swelling accompanying the diffusion of sucrose towards the matrix, typical of pore opening. If ruthenium red is omitted no absorbance change takes place (traces b in both panels). As previously reported [23], addition of 100 μM spermine after ruthenium red and before FCCP (trace c in panel A) induces an inhibitory effect (90%) that is the maximum observed; in fact, a higher concentration (trace d in panel A) does not enhance the inhibition. In this latter

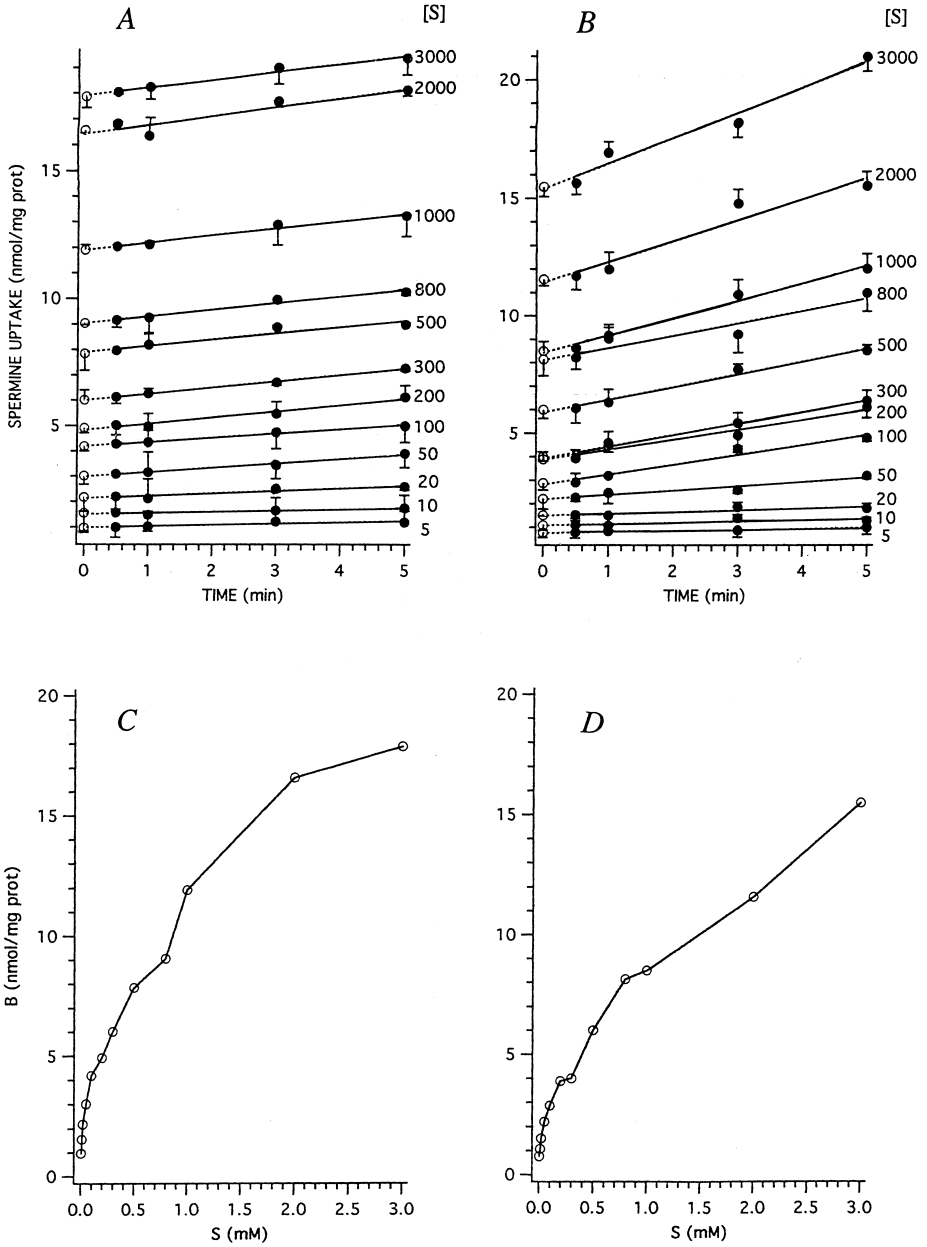

Fig. 2. Concentration-dependent spermine uptake by mitochondria deenergized by FCCP (panels A and C) or antimycin A (panels B and D). RLM were incubated in standard medium as described in Section 2. The zero time reported in the plot of panels A and B corresponds to the addition time of different [^{14}C]spermine concentrations [*S*] in the range of 5–3000 μM (0.05 μCi/ml) as indicated along the curves. These additions were made together with 0.2 μM FCCP (panel A) or 45 nM antimycin A (panel B). Ruthenium red (1 μM) was added in all the experiments 90 s after RLM and 30 s before the addition of spermine and deenergizer. Open circles report the amount of spermine that binds instantaneously at zero time. The results represent the mean value of 10 experiments. Panels C and D report zero-time spermine binding as the function of total spermine concentration. The curves were drawn using zero-time bound spermine values [*B*] calculated by extrapolation of data from the experiments shown in panels A and B. Total spermine concentrations [*S*] are the same as those reported in panels A and B.

case no decrease in the initial absorption of the suspension, which would indicate mitochondrial aggregation, was observed. Mitochondria undergo a similar swelling upon substitution of FCCP with antimycin A (trace a in panel B). Addition of 100 μM spermine also induces the maximum inhibitory effect on the absorbance decrease in the presence of antimycin A (trace c in panel B), but to a lesser extent (80%) compared to previous experiments performed using FCCP (compare this trace with trace c in panel A). This difference in the extent of inhibition in the presence of the two agents is also observed if spermine is added to the reaction mixture prior to mitochondria (results not reported). Using these mitochondrial preparations, the permeability transition can also be achieved in the usual way by incubating mitochondria with 100 μM Ca^{2+} plus 3 mM phosphate, without ruthenium plus FCCP or antimycin A (see inset in Fig. 1, trace a). In this case, as previously reported [26], 50 μM spermine is sufficient to completely block matrix swelling (inset in Fig. 1, trace b). The same maximum extent of inhibition of swelling exhibited by 100 μM spermine (90% with FCCP and 80% with antimycin A) has also been

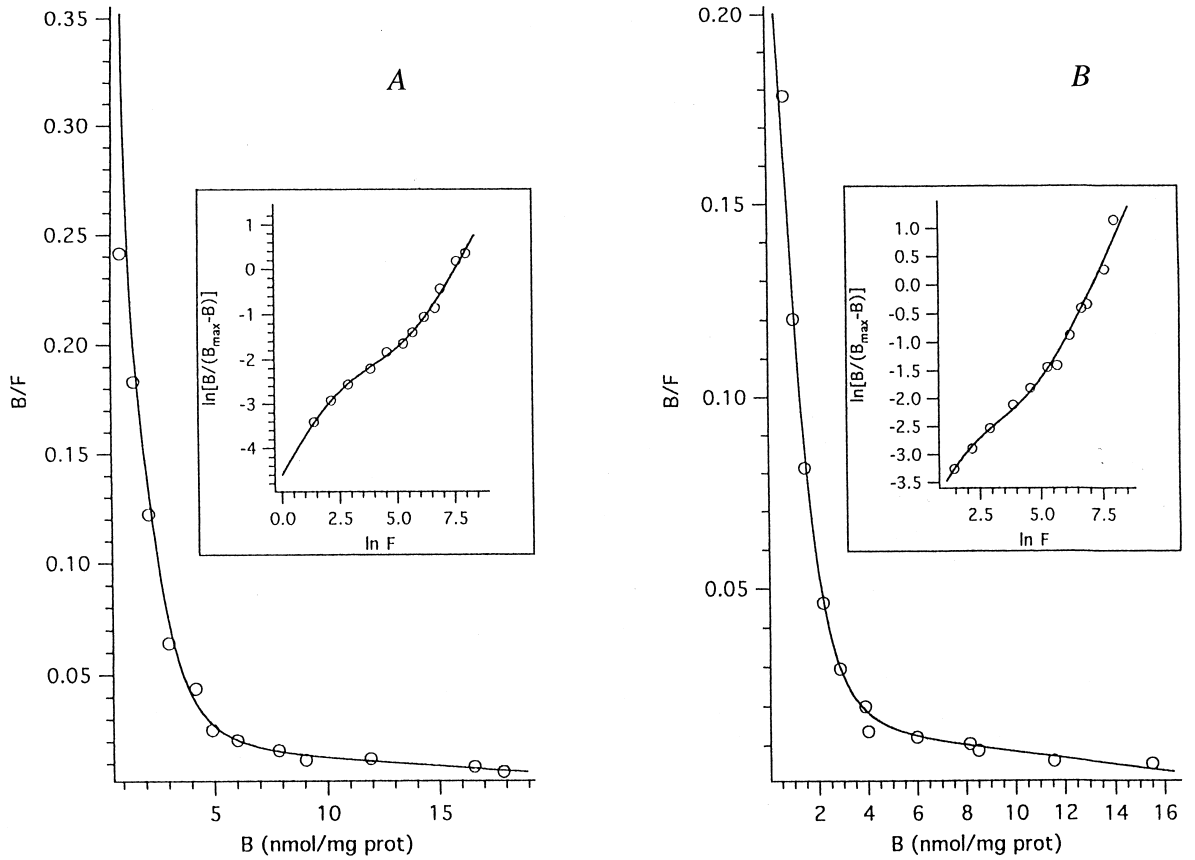

Fig. 3. Spermine binding analysis in the presence of FCCP (panel A) or antimycin A (panel B), with the thermodynamic treatment of Scatchard. The insets report the corresponding analysis with the treatment of Hill. The experimental data (open circles) were calculated as follows: bound spermine values B were as reported in Fig. 2; free spermine concentration F was calculated by subtracting bound spermine B from total spermine concentration [S] as reported in Fig. 2. The continuous lines represent the theoretical best fitting curves whose corresponding equations are derived from general Eq. 1) for Scatchard analysis and Eq. 2 for Hill analysis (see Section 2 and [33,34]).

observed by evaluating two other events associated with permeability transition induction, i.e. Mg^{2+} efflux and sucrose uptake (data not shown).

Fig. 2 shows the uptake of spermine by mitochondria incubated in standard medium in the presence of ruthenium red and deenergized with either FCCP (panel A) or antimycin A (panel B). Twelve spermine concentrations, ranging from 5 to 3000 μM, were tested. In this experiment, after an initial rapid binding, a very modest uptake of the polyamine is observed under both deenergizing conditions; this uptake takes place only during the first 5 min of the reaction. The rate of uptake depends on both the spermine concentration and the deenergizing agent used and is considerably higher in the presence of antimycin A (panel B). The different aliquots of spermine that bind to the mitochondrial membrane at zero time are calculated by extrapolation on the y-axis (see dotted line segments and open circles). Details of the experimental approach used to measure spermine uptake at zero time are provided in [34].

Table 1
Spermine binding parameters in deenergized mitochondria; a comparison with energized mitochondria

	B_{max} (nmol/mg protein)	B_{max1} (nmol/mg protein)	B_{max2} (nmol/mg protein)	$K_{1,1}$ (mol/l)	$K_{2,1}$ (mol/l)	β_1 (mg protein/nmol)	χ^b
Mitochondria deenergized by FCCP	30.32 (9)[a]	2.97 (3)	27.35 (6)	88.5 (5)$\times 10^{-6}$	2000 (21)$\times 10^{-6}$	0.101 (2)	0.0410
Mitochondria deenergized by ant. A	25.66 (6)	2.35 (2)	23.31 (4)	74.6 (5)$\times 10^{-6}$	16.77 (4)$\times 10^{-6}$	0.160 (3)	0.0387
Energized mitochondria[c]	23.08 (4)	8.29 (2)	14.79 (2)	42.3 (3)$\times 10^{-6}$	909 (12)$\times 10^{-6}$	0.161 (3)	0.0339

[a]Standard deviations in the least significant digits are given in parentheses.
[b]χ indicates the goodness of fit.

$$\chi = \frac{\sum |(N_o)-(N_c)|}{\sum |(N_c)|},$$

where (N_o) is the experimental value and (N_c) is the calculated value. For a Scatchard plot, N is given by B/F and for a Hill plot by $\ln[B/(B_{max}-B)]$.
[c]Data reported from [34].

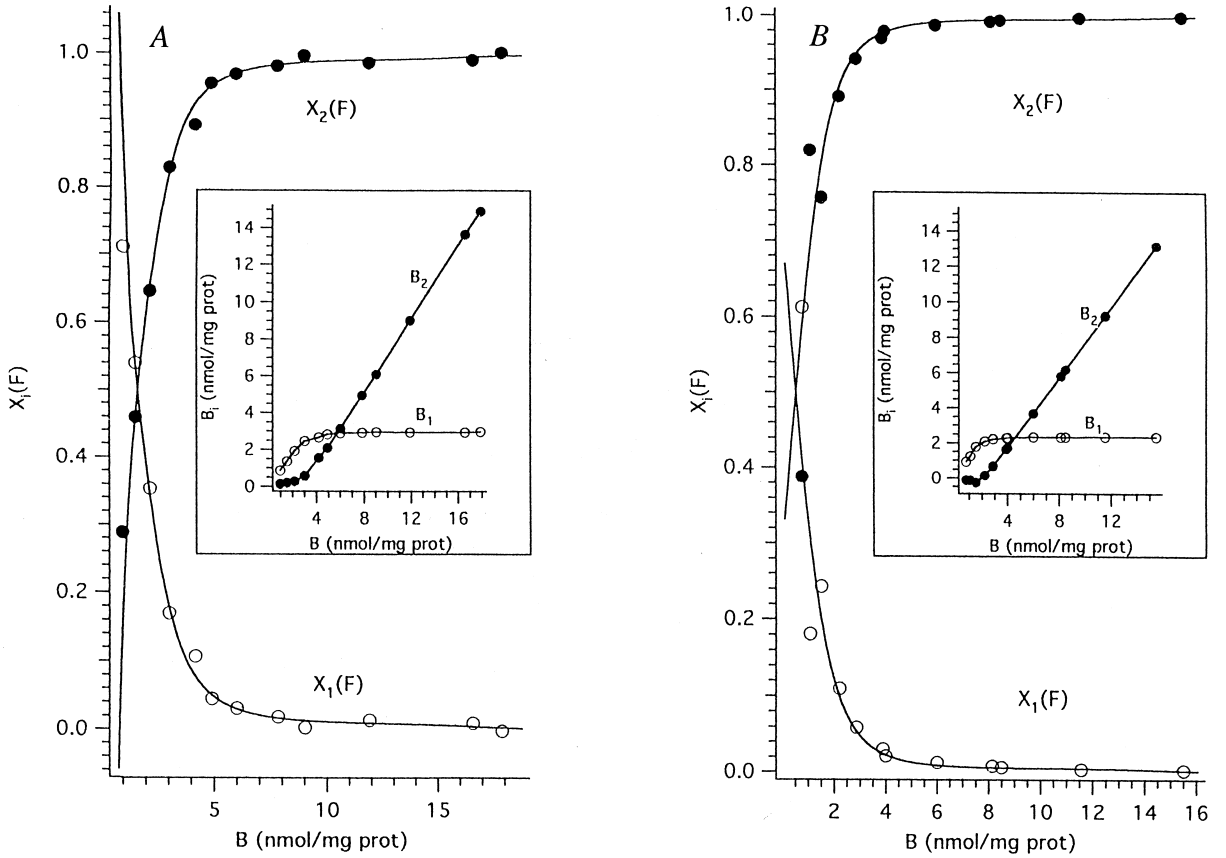

Fig. 4. Molar fraction ratio of spermine binding to mitochondria deenergized by FCCP (panel A) or antimycin A (panel B). The calculations refer to the amount of spermine required to fill the binding sites. $X_1(F)$ and $X_2(F)$ are the molar fraction ratios required to fill the first (S_1) and the second (S_2) spermine binding site, respectively. The insets report the subdivision of total bound spermine between the S_1 and S_2 sites. The two aliquots, B_1 and B_2, bound to S_1 and S_2 sites respectively, were determined by Eq. 3, using the molar fraction ratio $X_1(F)$ and $X_2(F)$ of zero-time bound spermine and B_{max1} and B_{max2} values reported in Table 1. An example of this calculation is reported in Fig. 3 of [34].

The amount of spermine bound at zero time, B, is plotted as the function of total spermine concentration [S], generating the diagrams B/S reported in panel C (FCCP-treated) and panel D (antimycin A-treated).

Fig. 3 shows spermine binding analyses obtained by using the thermodynamic treatments of Scatchard and Hill [33] as previously reported for energized mitochondria [34]. Binding data, plotted as dependence of B/F on B and ln $[B/(B_{max}-B)$ on ln F, are simulated with two series of curve profiles belonging to Eqs. 1 and 2, obtained by computer simulations for several parameters S and n_i (see Section 2). The theoretical curves that satisfactorily fit the experimental binding data obtained in the presence of FCCP (panel A) or antimycin A (panel B) are typical for two binding sites, S_1 and S_2, both with monocoordination.

Table 1 reports spermine binding parameters of deenergized mitochondria obtained by using both the Scatchard and the Hill data representation methods. For purposes of comparison this table also reports the same parameters previously determined for energized mitochondria (see [34]). This analysis demonstrates the presence of two monocoordinated binding sites on the membranes of deenergized mitochondria, as found in energized mitochondria [34]. The total binding capacity in the presence of FCCP is 30.32 nmol/mg protein, with 10% and 90% distributed between the S_1 and S_2 sites respectively. The dissociation constants $K_{1,1}$ and $K_{2,1}$ of sites S_1 and S_2, respectively, demonstrate that the affinity of S_1 is about 22.5 times higher than that of S_2. The total spermine binding capacity in the presence of antimycin A is 25.66 nmol/mg protein, with 9% and 91% distributed between the S_1 and S_2 sites, respectively. The dissociation constants $K_{1,1}$ and $K_{2,1}$ demonstrate that S_2 has a higher affinity than S_1, i.e. opposite to the affinities measured in the presence of FCCP. The main difference arising from the comparison of binding parameters reported in Table 1 is that under deenergization conditions spermine is largely bound to the S_2 site. Furthermore, the dissociation constants undergo different variations depending on the deenergizing agent. With FCCP, the spermine binding

Table 2
Distribution of total bound spermine to S_1 and S_2 sites in deenergized mitochondria

		Bound spermine (nmol/mg protein)		
		Total	S_1	S_2
+FCCP	100 μM SPM	4	2.6	1.4
	250 μM SPM	5.35	2.97	2.38
+Antimycin A	100 μM SPM	2.8	2.1	0.7
	250 μM SPM	4.0	2.35	1.65

Total bound spermine values were calculated from the data as in Fig. 2. The distribution between S_1 and S_2 sites was calculated by means of the molar fraction ratio of spermine binding, reported in Fig. 4.

affinity diminishes at both sites by about two-fold. With antimycin A, the binding affinity decreases at S_1 and increases at S_2 by about 2- and 50-fold, respectively. Parameter β_1, which describes the possible influence of the parallel filling of S_2 on filling of S_1, is determined by Eq. 3 (see Section 2) and does not exhibit any difference between deenergized and energized mitochondria.

Fig. 4 shows the molar fraction ratios $X_1(F)$ and $X_2(F)$ for the aliquot of free spermine that can bind to sites S_1 and S_2, respectively, determined in the presence of FCCP (panel A) or antimycin A (panel B). The values are obtained by using parameter β_1 reported in Table 1. As previously observed for energized mitochondria [34], these calculations show that with increasing amounts of bound spermine, $X_1(F)$ decreases in the presence of both deenergizing agents and, conversely, $X_2(F)$ increases. This signifies that the S_1 site is filled before the S_2 site. However, as demonstrated in the insets of Fig. 4, the S_2 site begins to bind spermine before the S_1 site is filled; this result was not observed in previous experiments [34].

Table 2 reports the distribution of membrane-bound spermine on sites S_1 and S_2 in the presence of either FCCP or antimycin A, measured using two polyamine concentrations (100 or 250 μM). The table emphasizes that the values of the S_1 site are at saturation at 250 μM spermine.

4. Discussion

The results of the present study demonstrate that besides protecting against the permeability transition induced in liver mitochondria by ruthenium red plus FCCP [23] (Fig. 1, panel A), spermine is also able to inhibit the phenomenon when it is induced by ruthenium red plus antimycin A (Fig. 1, panel B). The polyamine is considerably more effective in inhibiting the permeability transition when the phenomenon is induced by ruthenium red plus FCCP (compare the two panels in Fig. 1).

Furthermore, the data reported here point out that both deenergizing agents decrease the capacity of spermine to inhibit the permeability transition. In fact, by comparing the effect of spermine on the swelling of deenergized mitochondria (panels A and B in Fig. 1) and initially energized mitochondria (inset in Fig. 1), it is evident that the polyamine is fully inhibitory only in the latter case.

The results reported in Fig. 2, panels A and B, show that under the conditions in which spermine strongly inhibits the permeability transition, only a small proportion of the polyamine is taken up by deenergized mitochondria. The effect is slightly more pronounced in the presence of antimycin A (panel B). This fact could be ascribed to either an imperfect or delayed pore closure due to the presence of the deenergizing agents, which permits a low level of polyamine uptake. Very probably the latter proposal is more plausible, as after 7 min of incubation, no polyamine uptake is yet observable (data not shown).

Another difference between the mitochondria-spermine interactions in the presence of the two deenergizing agents is emphasized by comparing panels C and D of Fig. 2. The B/S diagrams show that zero time spermine binding is considerably higher with FCCP than with antimycin A, yielding noticeably different curve shapes. These results demonstrate that the deenergizing agents act on mitochondrial spermine binding via different mechanisms.

By using a new thermodynamic treatment of ligand-receptor interactions [33], it has recently been demonstrated that energized mitochondria contain two independent spermine binding sites, S_1 and S_2, both with monocoordination and low affinity and high binding capacity, located on the outer membrane and/or on the external surface of the inner membrane [34]. As proposed in the previous study, binding of spermine to the S_1 site would be competent for the prevention of the permeability transition and polyamine transport into the matrix. The S_2 site may be involved in the activation of mitochondrial Ca^{2+} uptake [36] and possibly in other activities such as the spermine-dependent mitochondrial transport of some cytosolic enzymes [37,38]. Different functions for the two mitochondrial spermine binding sites have also been proposed by other authors [36].

The thermodynamic model analysis of spermine binding in deenergized mitochondria clearly demonstrates that FCCP and antimycin A promote a remarkable perturbation of both binding sites. These deenergizing agents induce a strong reduction in S_1 binding and a strong enhancement in S_2 binding (see Table 1). The very low β_1 values, similar to those calculated in energized condition, demonstrate that the filling of both sites is not reciprocally influenced (Table 1).

The reduced binding capacity of the S_1 site in the presence of FCCP or antimycin A could account for the incomplete or delayed protective action exhibited by spermine (see Fig. 1, panels A and B), compared with the total inhibition of the permeability transition induced in the usual way (see inset in Fig. 1),. As reported in this figure, 100 μM spermine produced the maximum extent of inhibition of the permeability transition (i.e. 90% and 80% inhibition in FCCP and antimycin A treated samples, respectively). Very probably, at this external concentration the amounts of spermine bound to site S_1 (i.e. 2.6 and 2.1 nmol/mg protein in the presence of FCCP and antimycin A, respectively; see Table 2) are not sufficient to completely inhibit the permeability transition, given that at least 3 nmol/mg protein are necessary to obtain complete protection in energized mitochondria [34]. Furthermore, these results can also explain the different protective effects exhibited by spermine in the presence of the two deenergizing agents. In fact, spermine is less effective when the permeability transition is induced by antimycin A than in the presence of FCCP (compare panels A and B in Fig. 1). It is also possible that, besides decreasing the spermine binding capacity, FCCP and antimycin A affect the intrinsic properties of the S_1 site. This is supported by the observation that raising the spermine concentration to 250 μM or higher does not augment its inhibition of the permeability transition (i.e. 90% and 80% protection in the presence of FCCP and antimycin A, respectively, Fig. 1). At these spermine concentrations the S_1 site is saturated with 2.97 nmol/mg protein in the presence of FCCP and 2.35 nmol/mg protein in the presence of antimycin A (see Table 2) but this does not translate to better protection.

The enhancement of spermine binding capacity observed at the level of the S_2 site may somehow be connected to the large quantities of casein kinase I and casein kinase II enzymes taken up by mitochondrial membranes under these conditions (manuscript in preparation). This fact may have important implications for the enzymes' regulation during spermine-pore interactions. Furthermore, this site could be involved in the release, mediated by the polyamine, of mersalyl-inhibited phosphate carrier in mitochondria deenergized by FCCP

[39]. The high spermine concentration (1 mM) necessary to reactivate this transporter supports this hypothesis.

The reported results do not allow us to infer whether the observed perturbations in spermine binding sites are due to a direct effect of the deenergizing agents or to membrane depolarization or both. We hypothesize that the change in binding capacity and the decreased binding affinity are due to membrane depolarization that affects the normal charge orientation present in the two sites at physiological $\Delta\Psi$. The different spermine binding parameters obtained in the presence of FCCP and antimycin A could account for the lower degree of deenergization induced by antimycin A [40]. Instead, the particular aliquot distributions of spermine and its increased binding affinity at the S_2 site induced by antimycin A could be ascribed to a direct effect of the molecule.

It was suggested that the transition pore plays an important role in cell physiology and pathophysiology, that is, in intracellular signal transduction [41], in the control of energy wasting [1], in many types of cell injury [42,43] and in apoptosis [44]. If we assume that the deenergization achieved in the presence of ruthenium red plus either FCCP or antimycin A simulates events occurring in vivo when particular conditions, e.g. anoxia [45], trigger the permeability transition, the reported results support our belief that spermine plays a central physiological role in modulating this phenomenon.

Acknowledgements: The authors are grateful to Mr. Mario Mancon, Dr. Michela Campagnolo and Dr. Cinzia Tessarin for their skilful technical assistance. The authors also wish to thank Prof. Ludovico Sartorelli for reading the paper and helpful discussions.

References

[1] Gunter, T.E. and Pfeiffer, D.R. (1990) Am. J. Physiol. 258, C755–C786.
[2] Zoratti, M. and Szabò, I. (1995) Biochim. Biophys. Acta 1241, 139–176.
[3] Crompton, M., Ellinger, H. and Costi, A. (1988) Biochem. J. 255, 357–360.
[4] Novgorodov, S.A., Gudz, T.I., Kushnareva, Y.E., Zorov, D.B. and Kudrjashov, Y.B. (1990) FEBS Lett. 270, 108–110.
[5] Bernardi, P., Veronese, P. and Petronilli, V. (1993) J. Biol. Chem. 268, 1005–1010.
[6] Halestrap, A.P. and Davidson, A.M. (1990) Biochem. J. 268, 153–160.
[7] Szabò, I. and Zoratti, M. (1992) J. Bioenerg. Biomembr. 24, 111–117.
[8] Petronilli, V., Cola, C. and Bernardi, P. (1993) J. Biol. Chem. 268, 1011–1016.
[9] Szabò, I. and Zoratti, M. (1993) FEBS Lett. 330, 206–210.
[10] Szabò, I., De Pinto, V. and Zoratti, M. (1993) FEBS Lett. 330, 201–205.
[11] Beutner, G., Rück, A., Riede, B., Welte, W. and Brdiczka, D. (1996) FEBS Lett. 396, 189–195.
[12] Nicolli, A., Basso, E., Petronilli, V., Wenger, R.M. and Bernardi, P. (1995) J. Biol. Chem. 271, 2185–2192.
[13] Jurkowitz, M.S., Geisbulher, T., Jung, D.W. and Brierley, G.P. (1983) Arch. Biochem. Biophys. 223, 120–128.
[14] Igbavboa, U. and Pfeiffer, D.R. (1991) Biochim. Biophys. Acta 1059, 339–347.
[15] Vasington, F.D., Gazzotti, P., Tiozzo, R. and Carafoli, E. (1972) Biochim. Biophys. Acta 256, 43–54.
[16] Pozzan, T., Bragadin, M. and Azzone, G.F. (1977) Biochemistry 16, 5618–5625.
[17] Fiskum, G. and Cockrell, R.S. (1978) FEBS Lett. 92, 125–128.
[18] Bernardi, P. (1992) J. Biol. Chem. 267, 8334–8339.
[19] Igbavboa, U. and Pfeiffer, D.R. (1988) J. Biol. Chem. 263, 1405–1412.
[20] Tassani, V., Campagnolo, M., Toninello, A. and Siliprandi, D. (1996) Biochem. Biophys. Res. Commun. 226, 850–854.
[21] Toninello, A., Di Lisa, F., Siliprandi, D. and Siliprandi, N. (1984) in: Advances in Polyamines in Biomedical Sciences (Caldarera, C.M. and Bachrach, U., Eds.), pp. 31–36, CLUEB, Bologna.
[22] Siliprandi, N., Siliprandi, D., Toninello, A. and Garlid, K.D. (1988) in: Molecular Basis of Biomembrane Transport (Palmieri, F. and Quagliarello, E., Eds.), pp. 155–162, Elsevier, Amsterdam.
[23] Lapidus, R.G. and Sokolove, P.M. (1993) Arch. Biochem. Biophys. 306, 246–253.
[24] Rigobello, M.P., Toninello, A., Siliprandi, D. and Bindoli, A. (1993) Biochem. Biophys. Res. Commun. 194, 1276–1281.
[25] Lapidus, R.G. and Sokolove, P.M. (1994) J. Biol. Chem. 269, 18931–18936.
[26] Tassani, V., Biban, C., Toninello, A. and Siliprandi, D. (1995) Biochem. Biophys. Res. Commun. 207, 661–667.
[27] Toninello, A., Dalla Via, L., Testa, S., Siliprandi, D. and Siliprandi, N. (1990) Cardioscience 1, 287–294.
[28] Lapidus, R.G. and Sokolove, P.M. (1992) FEBS Lett. 313, 314–318.
[29] Toninello, A., Siliprandi, D. and Siliprandi, N. (1982) FEBS Lett. 142, 63–66.
[30] Toninello, A., Miotto, G., Siliprandi, D., Siliprandi, N. and Garlid, K.D. (1988) J. Biol. Chem. 263, 19407–19411.
[31] Toninello, A., Dalla Via, L., Siliprandi, D. and Garlid, K.D. (1992) J. Biol. Chem. 267, 18393–18397.
[32] Toninello, A., Di Lisa, F., Siliprandi, D. and Siliprandi, N. (1985) Biochim. Biophys. Acta 815, 399–404.
[33] Di Noto, V., Dalla Via, L., Toninello, A. and Vidali, M. (1996) Macromol. Theory Simul. 5, 165–181.
[34] Dalla Via, L., Di Noto, V., Siliprandi, D. and Toninello, A. (1996) Biochim. Biophys. Acta 1284, 247–252.
[35] Broekemeier, K.M. and Pfeiffer, D.R. (1995) Biochemistry 34, 16440–16449.
[36] Rustenbeck, I., Reiter, H. and Lenzen, S. (1996) Biochem. Mol. Biol. Int. 38, 1003–1011.
[37] Bordin, L., Cattapan, F., Clari, G., Toninello, A., Siliprandi, N. and Moret, V. (1994) Biochim. Biophys. Acta 1199, 266–270.
[38] Clari, G., Toninello, A., Bordin, L., Cattapan, F., Piccinelli-Siliprandi, D. and Moret, V. (1994) Biochem. Biophys. Res. Commun. 205, 389–395.
[39] Toninello, A., Di Lisa, F., Siliprandi, D. and Siliprandi, N. (1986) Arch. Biochem. Biophys. 245, 363–368.
[40] Murphy, M.P. and Brand, M. (1988) Eur. J. Biochem. 173, 637–644.
[41] Evtodienko, Y.V., Teplova, V., Khavaja, J. and Saris, N.E. (1994) Cell Calcium 15, 143–152.
[42] Brown, R.H. (1995) Curr. Opin. Neurol. 8, 373–378.
[43] Westendorp, M.O., Shatrov, V.A., Schulze-Ostoff, K., Frank, R., Kraft, M., Los, M., Krammer, P.H., Droge, W. and Lehmann (1995) EMBO J. 14, 546–554.
[44] Kroemer, G., Petit, P., Zamzami, N., Vayssiere, J.L. and Mignotto, B. (1995) FASEB J. 9, 1277–1288.
[45] Pastorino, J.G., Snyder, J.W., Serroni, A., Hock, J.B. and Farber, J.L. (1993) J. Biol. Chem. 268, 13791–13796.